

# Global fitting analysis on cosmological models after BICEP2

Hong Li,<sup>1,\*</sup> Jun-Qing Xia,<sup>1</sup> and Xinmin Zhang<sup>2</sup>

<sup>1</sup>*Key Laboratory of Particle Astrophysics, Institute of High Energy Physics, Chinese Academy of Science, P.O.Box 918-3, Beijing 100049, P.R.China*

<sup>2</sup>*Theoretical Physics Division, Institute of High Energy Physics, Chinese Academy of Science, P.O.Box 918-4, Beijing 100049, P.R.China*

Recently, BICEP2 collaboration has released their results on the measurements of the CMB polarizations. In the framework of the  $\Lambda$ CDM with a power law form of the scalar primordial power spectrum, this new measurement on the B-mode puts a tight constraint on tensor/scalar ratio  $r = 0.2_{-0.05}^{+0.07}$  ( $1\sigma$ ), which however is in tension with the Planck limit,  $r < 0.11$  (95% C.L.). In this paper, we consider various extensions of the  $\Lambda$ CDM model by introducing extra cosmological parameters such as the equation state of dark energy  $w$ , the curvature of the universe  $\Omega_k$ , the running of the scalar power spectrum index  $\alpha_s$ , the sum of the neutrino mass  $\Sigma m_\nu$ , the effective number of neutrinos  $N_{eff}$ , the tensor power spectrum index  $n_t$ , then perform the global fit to the BICEP2, Planck and also the SN and BAO data. Our results show the cosmological parameters  $\alpha_s$  and  $n_t$  are highly and directly correlated with the tensor/scalar ratio  $r$ . However indirectly the parameters  $\Omega_k$  and  $N_{eff}$  are also correlated with  $r$ . We will in this paper give the numerical values on the parameters introduced and show explicitly how the tension between the BICEP2 and Planck is effectively alleviated by the inclusion of the parameters  $\Omega_k$ ,  $\alpha_s$ ,  $N_{eff}$  and  $n_t$  separately.

PACS numbers: 98.80.Es, 98.80.Cq

## I. INTRODUCTION

Recently, the BICEP2 collaboration announced that they have detected the primordial tensor perturbation modes at more than  $7\sigma$  confidence level, and it is the most accurate measurements on the cosmic microwave background (CMB) B-mode polarization at current stage. Basing on the data, within the framework of a power-law  $\Lambda$ CDM, BICEP2 collaboration gives a tight constraint on the tensor/scalar ratio as  $r = 0.2_{-0.05}^{+0.07}$ [1]. This is the first time that data sets a lower bound on the primordial tensor modes and is the most accurate constraints on tensor/scalar ratio. The detection of the primordial tensor perturbations plays a crucial and important role in understanding the early universe and diagnosing inflation models. The BICEP2 measurements of CMB polarization power spectrum has a series of interesting implications on cosmological models [3–12].

The tensor/scalar ratio  $r = 0.2_{-0.05}^{+0.07}$  however is in tension with the previous constraint from the Planck[2]temperature power spectrum,  $r < 0.11$  ( $2\sigma$ ). Considering that the tension is given by fitting the data within the framework of a power-law  $\Lambda$ CDM model, a more general data fitting analysis might be possible to provide a way to alleviate the tension of the two CMB data. In fact, the BICEP2 collaboration in their paper[1] has pointed out already that including a running of the scalar power spectrum index makes both BICEP2 and Planck consistent. The reason for this is the degeneracies among the cosmological parameters. In paper[13] we have performed a detailed study on the impacts of the degeneracies on the determination of the cosmological parameters. Interestingly we also found the 95% upper limit on  $r$  changes from 0.15 in the power-law  $\Lambda$ CDM model to 0.37 when including the running parameter  $\alpha_s$ . This result obtained from the fitting with the previous CMB WMAP7 data together with SN + BAO + HST gives a weak constraint on  $r$ , however our analysis shows explicitly how the upper limit of  $r$  gets relaxed when including the running parameter  $\alpha_s$ . Last year, when Planck released their data, their measured value of Hubble constant  $H_0$  is shown to be in tension with some other measurements given by the lower-redshift methods, such as the direct  $H_0$  probe from the Hubble Space Telescope (HST) observations of Cepheid variables[16, 17]. In Refs. [14, 15], by making use of the parameter degeneracies we have shown that introducing the EoS parameter of dark energy into the data fitting analysis can be helpful for reconciling this tension on  $H_0$ . Along this line, in this paper we examine the tension on  $r$  between BICEP2 and Planck in various extensions of the power law  $\Lambda$ CDM model by introducing extra cosmological parameters such as the equation state of dark energy  $w$ , the curvature of the universe  $\Omega_k$ , the running of the scalar power spectrum index  $\alpha_s$ , the sum of the neutrino mass  $\Sigma m_\nu$ , the effective number of neutrinos  $N_{eff}$ , the tensor power spectrum index  $n_t$ , then perform the global fit. Our results show that the inflationary parameters  $n_t$

---

\*Electronic address: hongli@ihep.ac.cn

and  $\alpha_s$  can be helpful for reconciling the tension. By doing the fitting analysis, we find that  $r$  is negatively correlated with  $\alpha_s$ , and the correlation coefficient is around  $-0.35$ . The correlation between  $r$  and  $n_t$  is highly scale dependent, for pivot scale  $k_{pt} = 0.05 \text{Mpc}^{-1}$ , they are positively correlated and the coefficient is  $0.78$ . So for models  $\Lambda\text{CDM} + r + n_t$  and  $\Lambda\text{CDM} + r + \alpha_s$ , our results show the tension can be remarkably reconciled. Our results also show that even though  $N_{eff}$  and  $\Omega_k$  are weakly correlated with  $r$ , since they are correlated with  $n_s$ , they can also soften the tension in certain level.

The structure of our paper is organized as follows. In section II we will introduce the data sets we adopted in the fitting analysis and the global fitting procedure. In section III we present the constraints on various model parameters, and the discussion and summary are given in section IV.

## II. DATA SETS EMPLOYED AND GLOBAL FITTING ANALYSIS

### A. Numerical Method

We perform the global fitting of cosmological parameters using the CosmoMC package [18], a Markov Chain Monte Carlo (MCMC) code. The basic cosmological parameters are allowed to vary with top-hat priors: the cold dark matter energy density parameter  $\Omega_c h^2 \in [0.01, 0.99]$ , the baryon energy density parameter  $\Omega_b h^2 \in [0.005, 0.1]$ , the curvature term  $\Omega_k \in [-0.30, 0.3]$ , the effective numbers of neutrinos  $N_{eff} \in [0, 10]$ , the total neutrino mass  $\Sigma m_\nu \in [0, 1.5] eV$ , the scalar spectral index  $n_s \in [0.5, 1.5]$ , tensor index  $n_t \in [-4, 5]$ , tensor to scalar ratio  $r \in [0, 1]$ , the primordial amplitude  $\ln[10^{10} A_s] \in [2.7, 4.0]$ , the running of primordial scalar power spectrum index  $\alpha_s \in [-0.5, 0.5]$ , the ratio (multiplied by 100) of the sound horizon at decoupling over the angular diameter distance to the last scattering surface  $100\Theta_s \in [0.5, 10]$ , and the optical depth to reionization  $\tau \in [0.01, 0.8]$ . The pivot scale<sup>1</sup> is set at  $k_{s0} = 0.05 \text{Mpc}^{-1}$ . In our calculation, we assume an purely adiabatic initial condition.

The procedure of our study is the following. We start with the power law  $\Lambda\text{CDM} + r$  model described by the basic parameters

$$\{\Omega_b h^2, \Omega_c h^2, \Theta_s, \tau, n_s, A_s, r\} . \quad (1)$$

Then we consider various extensions of the model above by introducing the extra cosmological parameters: the equation state of dark energy  $w$ , the curvature of the universe  $\Omega_k$ , the running of the scalar power spectrum index  $\alpha_s$ , the sum of the neutrino mass  $\Sigma m_\nu$ , the effective number of neutrinos  $N_{eff}$  and the tensor power spectrum index  $n_t$ . And each time, we add only one new parameter for the fitting.

### B. Current Observational Data

In our analysis, we consider the following cosmological probes: i) power spectra of CMB temperature and polarization anisotropies released by Planck and polarization E and B modes given by BICEP2 collaborations; ii) the baryon acoustic oscillation in the galaxy power spectra; iii) luminosity distances of type Ia supernovae.

For the Planck data from the 1-year data release [2], we use the low- $\ell$  and high- $\ell$  CMB temperature power spectrum data from Planck with the low- $\ell$  WMAP9 [21] polarization data (Planck+WP). We marginalize over the nuisance parameters that model the unresolved foregrounds with wide priors [19], and do not include the CMB lensing data from Planck [20]. For the BICEP2 data sets, we adopt 9 bins of the E and B polarization field data sets in range of  $\ell[30, 150]^2$ .

Baryon Acoustic Oscillations provides an efficient method for measuring the expansion history by using features in the clustering of galaxies within large scale surveys as a ruler with which to measure the distance-redshift relation[23]. It measures not only the angular diameter distance,  $D_A(z)$ , but also the expansion rate of the universe,  $H(z)$ , which is powerful for studying dark energy [24]. Since the current BAO data are not accurate enough for extracting the information of  $D_A(z)$  and  $H(z)$  separately [25], one can only determine an effective distance [26]:

$$D_V(z) = [(1+z)^2 D_A^2(z) cz / H(z)]^{1/3} . \quad (2)$$

<sup>1</sup> For discussion on the scale dependence of  $n_t$  we choose another pivot scale of  $k_{s0} = 0.001 \text{Mpc}^{-1}$ .

<sup>2</sup> In the current study, we focus on the constraint on the primordial tensor perturbation, so have not included the POLARBEAR[22] results.

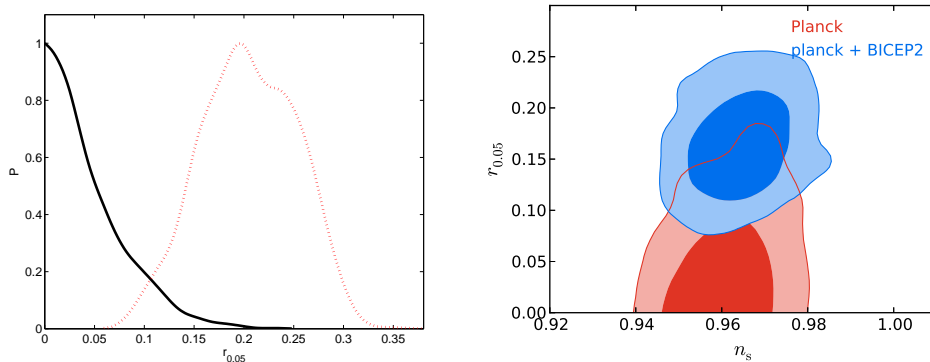


FIG. 1: The left panel: One-dimensional marginalized probability distribution of  $r$ . The red line is given by BICEP2 and the black line is given by Planck. The right panel: two-dimensional cross correlation between  $r$  and  $n_s$ .

TABLE I: We list the constraints on  $r$  and the new parameters introduced in extensions of the power law  $\Lambda$ CDM model from Planck+BICEP2 and also Planck only for comparison. The minimal  $\chi^2$  listed are for the corresponding models when fitting with Planck+BICEP2. The correlation coefficients indicated by (*corr*) show the correlation between  $r$  and the new parameter introduced in fitting with data sets of Planck+SN+BAO+BICEP2.

	$\Lambda$ CDM+ $r$	$\Lambda$ CDM+ $r+n_t$	$\Lambda$ CDM+ $r+\alpha_s$	$\Lambda$ CDM+ $r+N_{eff}$	$\Lambda$ CDM+ $r+\Omega_k$	$\Lambda$ CDM+ $r+\Sigma m_\nu$	$\Lambda$ CDM+ $r+w$
PLK+BICEP2	$r = 0.165 \pm 0.036$	$n_t = 0.79 \pm 0.21$	$\alpha_s = -0.027 \pm 0.01$	$N_{eff} = 4.03^{+0.43}_{-0.48}$	$\Omega_k = -0.055^{+0.051}_{-0.024}$	$\Sigma m_\nu < 0.616 \text{ eV}$	$w = -1.55^{+0.18}_{-0.34}$
PLK only	$r < 0.117$	<i>nolimit</i>	$\alpha_s = -0.221^{+0.011}_{-0.0009}$	$N_{eff} = 3.42 \pm 0.6$	$\Omega_k = -0.051^{+0.035}_{-0.028}$	$\Sigma m_\nu < 0.813 \text{ eV}$	$w = -1.509^{+0.226}_{-0.415}$
$\chi^2_{min}$	9853.3	9845	9846.7	9848.2	9847.0	9853.7	9853.6
<i>corr</i>	—	0.78	-0.35	0.05	-0.18	0.07	-0.03

Following the Planck analysis [2], in this paper we use the BAO measurement from the 6dF Galaxy Redshift Survey (6dFGRS) at a low redshift ( $r_s/D_V(z=0.106) = 0.336 \pm 0.015$ ) [27], and the measurement of the BAO scale based on a re-analysis of the Luminous Red Galaxies (LRG) sample from Sloan Digital Sky Survey (SDSS) Data Release 7 at the median redshift ( $r_s/D_V(z=0.35) = 0.1126 \pm 0.0022$ ) [28], and the BAO signal from BOSS CMASS DR9 data at ( $r_s/D_V(z=0.57) = 0.0732 \pm 0.0012$ ) [29].

Finally, we include data from Type Ia supernovae, which consists of luminosity distance measurements as a function of redshift,  $D_L(z)$ . In this paper we use the supernovae data set, “Union2.1” compilation, which includes 580 supernovae reprocessed by Ref.[30]. When calculating the likelihood, we marginalize the nuisance parameters, like the absolute magnitude  $M$ .

### III. CONSTRAINTS ON COSMOLOGICAL MODELS

We start to present our numerical results with only the CMB data. Within the power law  $\Lambda$ CDM model, we show in the left panel of figure 1 the one dimensional probability distribution of  $r$  given by fitting with Planck temperature and BICEP2 polarization E and B modes respectively. From Planck it gives  $r < 0.11$  ( $1\sigma$ ) and BICEP2 give  $r = 0.2^{+0.07}_{-0.05}$  ( $1\sigma$ ). We also show the comparison of the constraints in two dimensional plane of  $r$ - $n_s$  in the right panel of figure 1 and one can see that there’s no overlap for the two 68% confidence level contours.

Now we consider various extensions of the power law  $\Lambda$ CDM model. In table I, we list the constraints on the relevant parameters from Planck + BICEP2 and also the values from Planck only. For example, the constraints on the EoS of dark energy from BICEP2 + Planck is  $w = -1.55^{+0.18}_{-0.34}$ , and with Planck only,  $w = -1.509^{+0.226}_{-0.415}$ . This shows with BICEP2 + Planck, the errors get smaller and the central value of  $w$  becomes more negative. For the curvature of the universe,  $1\sigma$  limit is  $\Omega_k = -0.055^{+0.051}_{-0.024}$ , the total neutrino mass  $\Sigma m_\nu < 0.616 \text{ eV}$ , the effective number of neutrinos  $N_{eff} = 4.03^{+0.43}_{-0.48}$ , all of which are consistent and slightly tighten the constraints from Planck.

In figure 2, we show the two dimensional cross correlation between  $r$  and  $n_s$  in different models by fitting with Planck + BICEP2. We compare the models of  $\Lambda$ CDM +  $r + \alpha_s$ ,  $\Lambda$ CDM +  $r + N_{eff}$ , and  $\Lambda$ CDM +  $r + \Omega_k$  in the left

TABLE II: The constraints on tensor/scalar ratio  $r$  and the relevant extra cosmological parameters from Planck+SN+BAO with/without BICEP2. For Planck+SN+BAO we present the 95% C.L. upper limit, and for Planck+SN+BAO+BICEP2 we list the  $1\sigma$  constraints.

models	<i>Planck + SN + BAO</i>		<i>Planck + SN + BAO + BICEP2</i>	
$\Lambda$ CDM+ $r$	$r < 0.12$	–	$0.165^{+0.031}_{-0.040}$	–
$\Lambda$ CDM+ $r+n_t$	no-limit	$n_t > 0.296$	$r > 0.370$	$n_t = 0.822^{+0.240}_{-0.182}$
$\Lambda$ CDM+ $r+\alpha_s$	$r < 0.25$	$\alpha_s = -0.022 \pm 0.011$	$r = 0.199^{+0.037}_{-0.044}$	$\alpha_s = -0.0281 \pm 0.0099$
$\Lambda$ CDM+ $r+N_{eff}$	$r < 0.15$	$N_{eff} = 3.503^{+0.275}_{-0.274}$	$r = 0.169^{+0.031}_{-0.038}$	$N_{eff} = 3.678^{+0.299}_{-0.323}$
$\Lambda$ CDM+ $r+\Omega_k$	$r < 0.14$	$100\Omega_k = -0.0731 \pm 0.34$	$r = 0.173^{+0.035}_{-0.041}$	$100\Omega_k = -0.25 \pm 0.34$

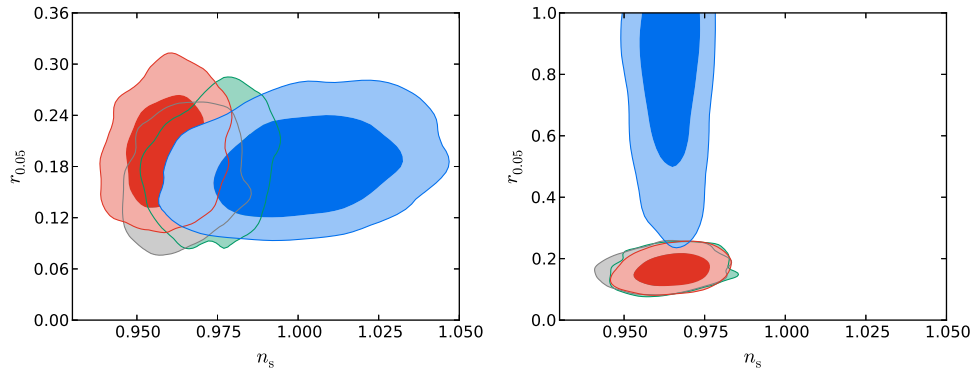


FIG. 2: The two-dimensional cross correlation between  $r$  and  $n_s$  by fitting with Planck + BICEP2. In the left panel we compare models of  $\Lambda$ CDM+ $r$  (gray),  $\Lambda$ CDM+ $r + \alpha_s$  (red),  $\Lambda$ CDM+ $r + N_{eff}$  (blue) and  $\Lambda$ CDM+ $r + \Omega_k$  (green), respectively. In the right panel we compare models of  $\Lambda$ CDM+ $r$  (green),  $\Lambda$ CDM+ $r + \Sigma m_\nu$  (gray),  $\Lambda$ CDM+ $r + w$  (red), and  $\Lambda$ CDM+ $r + n_t$  (blue), respectively.

panel, while in the right panel we compare  $\Lambda$ CDM +  $r + \Sigma m_\nu$ ,  $\Lambda$ CDM +  $r + w$  and  $\Lambda$ CDM +  $r + n_t$ . One can see clearly the effects of  $\alpha_s$ ,  $n_t$ ,  $N_{eff}$  and  $\Omega_k$ . However, for the parameters  $\Sigma m_\nu$  and  $w$ , the effects they can bring are minor. Thus in the study below, we will focus on the 4 types of models which corresponds to the inclusion of extra parameters of  $\alpha_s$ ,  $n_t$ ,  $N_{eff}$  and  $\Omega_k$ , respectively.

In order to get a tight constraint on the parameters, we now combine the CMB data with SN and BAO. We compare the 1 and  $2\sigma$  confidence contours in plane of  $r$ - $n_s$  for the 4 different cosmological models in figure 3 and table II. The contours in red are given by Planck + SN + BAO, while blue is given by Planck + SN + BAO + BICEP2.

Firstly, we study the effect from  $n_t$ . During the fitting procedure we free  $n_t$  and  $r$  simultaneously and ignore the inflation consistency relation  $n_t = -\frac{A_t}{8A_s}$ . We find that for the pivot scale  $k_{pivot} = 0.05$  the tensor index is positively correlated with  $r$ , and the correlation coefficient between them is about 0.78. Such a high correlation leads to a very weak constraint on both  $r$  and  $n_t$ , which one can see from Planck + SN + BAO. By taking into account the BICEP2 data, there's a lower limit on  $r$ , and  $r > 0.370$ , the constraint on  $n_t$  is  $n_t = 0.822^{+0.240}_{-0.182}$ . The constraints are pivot scale dependent. In figure 5 we plot the results with two pivot scales  $k_{pt} = 0.001 \text{ Mpc}^{-1}$  and  $k_{pt} = 0.004 \text{ Mpc}^{-1}$  for comparison. One can see for  $k_{pt} = 0.001 \text{ Mpc}^{-1}$ , we get constraints like  $r_{0.001} < 0.076$  and  $n_{t_{0.001}} = 1.04 \pm 0.39$ , and for  $k_{pt} = 0.004 \text{ Mpc}^{-1}$ , the constraints give  $r_{0.004} = 0.094 \pm 0.058$  and  $n_{t_{0.004}} = 0.94 \pm 0.76$ .

Then we consider the correlations between  $r$  and the running parameter  $\alpha_s$ . Our results are shown in the upper right panel of figure 3. The effect from the running is also sizable, as shown in the figure, since  $\alpha_s$  is negatively correlated with  $r$ . For a negative running which is preferred by the current data, a larger  $r$  can satisfy both Planck and BICEP2. In this case, we get  $r = 0.199^{+0.037}_{-0.044}$  with data sets of Planck+SN+BAO+BICEP2, and  $\alpha_s = -0.0281 \pm 0.0099$  which give a negative running of  $n_s$ . By comparing with  $\Lambda$ CDM +  $r$ , including the running parameter can decrease the minimal  $\chi^2$  of the fitting about 7, which indicates that  $\alpha_s$  can be helpful for balancing the two CMB data. In figure 4, we plot the expected TT and BB power spectra from the best fit models of  $\Lambda$ CDM+ $r$ ,  $\Lambda$ CDM+ $r + n_t$  as well as  $\Lambda$ CDM+ $r + \alpha_s$ . One can see from the BB power spectrum, the different models can account for the BICEP2 data equally well, but behave differently at small  $\ell$ , which can be distinguished by the future CMB measurements.

The effects from  $N_{eff}$  and  $\Omega_k$  are shown in the upper left panel and lower left panel of figure 3 respectively. We

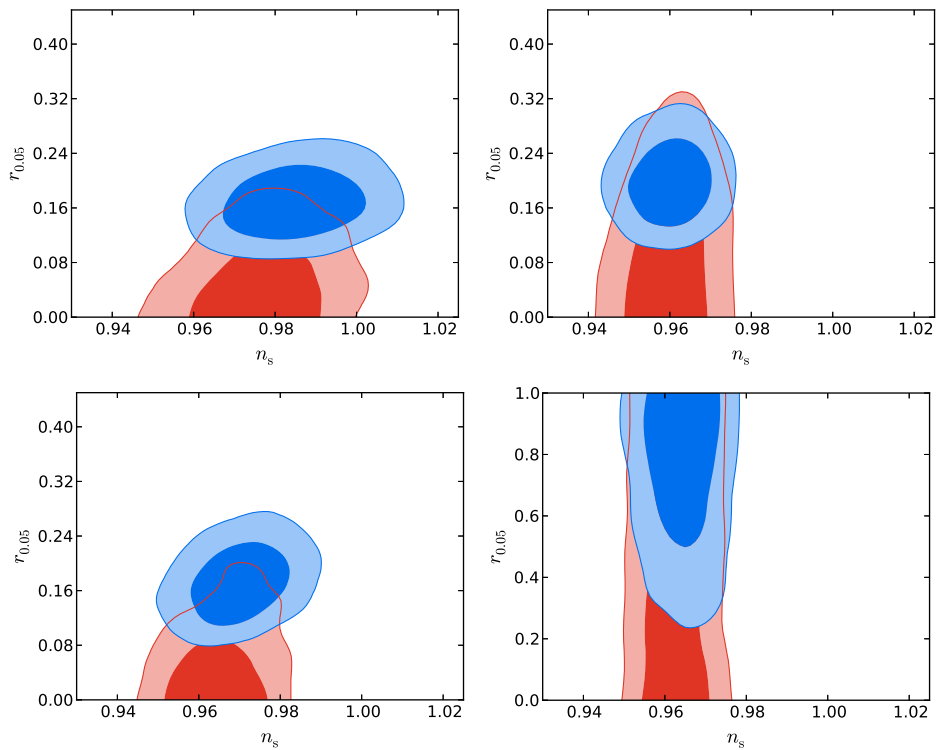


FIG. 3: Two-dimensional cross correlation between  $r$  and  $n_s$  by fitting with data sets of Planck + SN + BAO with (blue) and without (red) BICEP2. The panels are given by involving parameters  $N_{eff}$  (upper left),  $\alpha_s$  (upper right),  $\Omega_k$  (lower left) and  $n_t$  (lower right) respectively.

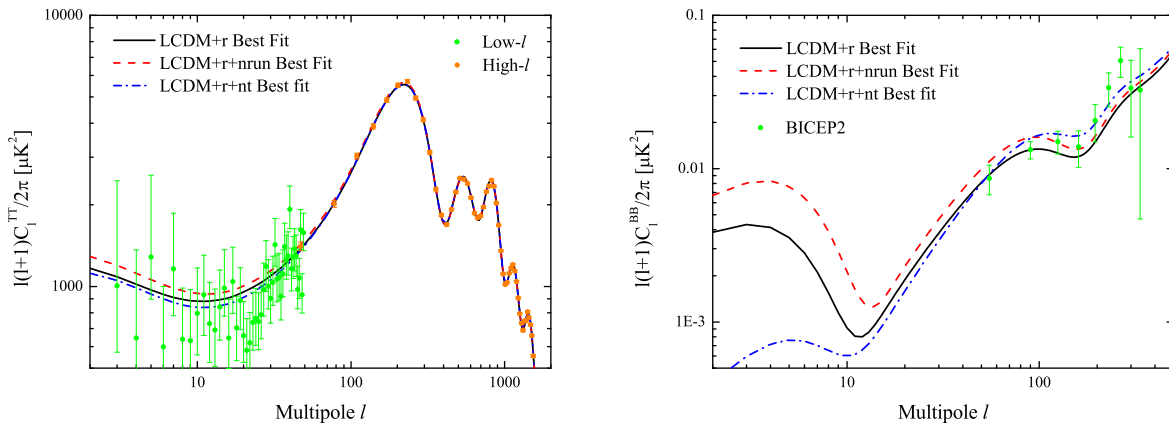


FIG. 4: Theoretical CMB TT (*Left*) and BB (*Right*) power spectra for the best fit  $\Lambda$ CDM+r,  $\Lambda$ CDM+r+n<sub>t</sub> and  $\Lambda$ CDM+r+ $\alpha_s$  models, as well as the Planck and BICEP2 observational data.

find that  $N_{eff}$  and  $\Omega_k$  are very weakly correlated with  $r$  and the coefficients are both around 0. However, they are strongly correlated with  $n_s$ , so they can indirectly affect the allowed parameter space. Our results show these two parameters can also be helpful to compromising the tension in certain level. Numerically we get  $r = 0.169_{-0.038}^{+0.031}$  and  $r = 0.173_{-0.041}^{+0.035}$  by introducing  $N_{eff}$  and  $\Omega_k$  respectively. And the constraints on  $N_{eff}$  and  $\Omega_k$  are  $N_{eff} = 3.678_{-0.323}^{+0.299}$  and  $100\Omega_k = -0.25 \pm 0.34$ , which are consistent with those from Planck and other observations.

Finally, we use the new BICEP2 data to study the rotation angle induced by the CPT-violating interaction [31].

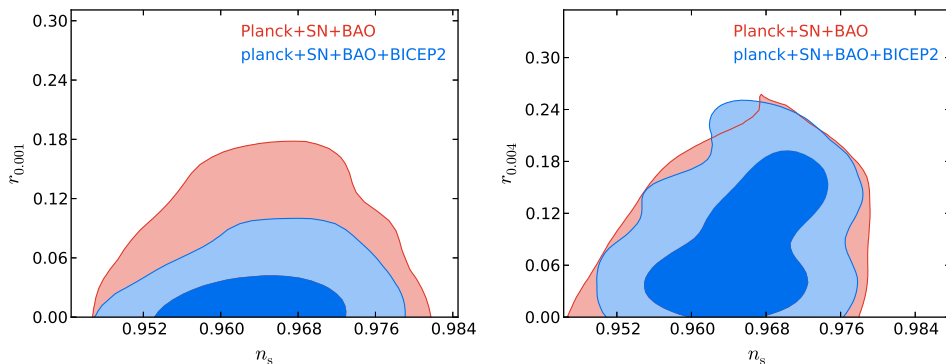


FIG. 5: Two-dimensional cross correlation constraints of  $r$  and  $n_s$  at pivot scales  $k_{pt} = 0.001\text{Mpc}^{-1}$  and  $k_{pt} = 0.004\text{Mpc}^{-1}$  by fitting with data sets of Planck + SN + BAO with (blue) and without (red) BICEP2.

Here, we only consider the isotropic rotation  $\alpha$  and leave the analysis on the direction-dependent rotation angle  $\alpha(\hat{\mathbf{n}})$  in the future work.

As we know, due to the non-zero rotation angle, the CMB polarization power spectra are modified. Especially, we have the non-zero CMB TB and EB cross power spectra, which vanish in the standard CMB theory. Therefore, we have used the published CMB TB and EB observational data, such as the WMAP and BICEP experiments, to constrain the rotation angle and test the CPT symmetry.

In 2010, the BICEP experiment published the two-year BICEP data, including the TB and EB information [32]. In ref. [33] we analysed this data and found that a non-zero rotation angle is favored at about  $2.4\sigma$  confidence level,  $\alpha = -2.60 \pm 1.02$  deg (68% C.L.), due to the clear bump structure in the BICEP TB and EB power spectra at  $\ell \sim 150$ . In 2013, the BICEP collaboration released the three-year data and re-analysed the constraint of the rotation angle [34]. They show when using the standard calibration method, the BICEP data still prefer a non-vanishing TB and EB power spectra with an overall polarization rotation  $\alpha = -2.77 \pm 0.86(\text{stat.}) \pm 1.3(\text{sys.})$  deg (68% C.L.), which still implies  $\alpha \neq 0$  at  $\sim 2\sigma$  confidence level [34, 35].

A sizable rotation angle will have an interesting effect on the CMB BB power spectrum (see Fig.4 of our paper in [33]). Here, in figure 6 we plot the CMB BB power spectra with several rotation angles. The BICEP2 BB data are also shown there. One can see a rotation angle  $\sim 4$  deg will generate a B mode with an amplitude at the order of magnitude comparable to the BICEP2. Some recent studies on the implications of rotation angle[36] on the BICEP2 results can be found in [37, 38].

In ref. [34] the authors proposed a new calibration method, “self-calibration”, in which they used the derived rotation angle to calibrate the detector polarization orientations. With the self calibration method, the rotation angle is minimized and the constraint on the tensor-to-scalar ratio  $r$  as shown in [34] becomes tighten from  $r < 0.70$  to  $r < 0.65$  at 95% confidence level. With the new BICEP2 data on EB and TB, we have analysed the rotation angle and obtained numerically  $\alpha = 0.12 \pm 0.16$  deg at the 68% C.L. which is expected and consistent with the use of “self calibration”. However it is curious to estimate how large the rotation angle could be before the “self calibration”. To do this, we recall BICEP2 collaboration in their paper ( see section 8.2) states they have done a rotation of  $\sim 1$  deg, based on which we obtain a conservative value of the rotation angle before self calibration which is  $\sim 0.88$  deg. Assuming the error 0.16 deg remains almostly the same before and after the self calibration, we estimate the rotation angle before the self calibration is around  $\alpha = 0.88 \pm 0.16$  deg which is non zero at more than  $5\sigma$  significance.

#### IV. SUMMARY AND DISCUSSION

Recently, the BICEP2 collaboration published their result on primordial tensor modes from the highest resolution E and B maps of the CMB polarization anisotropy. In the standard  $\Lambda$ CDM model, the BICEP2 data give a tight constraint on  $r$ , which prefers a larger tensor mode when comparing with the Planck temperature measurements. In this paper we have considered several extensions of the  $\Lambda$ CDM models, and found that 4 models by introducing extra cosmological parameters,  $n_t$ ,  $\alpha_s$ ,  $N_{eff}$  and  $\Omega_k$  can alleviate this tension. Furthermore, we have performed a detailed numerical calculation and fitted the model parameters to the BICEP2 + Planck + SN + BAO. On constraining the tensor index  $n_t$ , we find that it is pivot scale dependent, and with BICEP2 data, a blue tilt of the primordial gravitational waves spectrum can be allowed. Our study will be important to understand the resolution of the tension

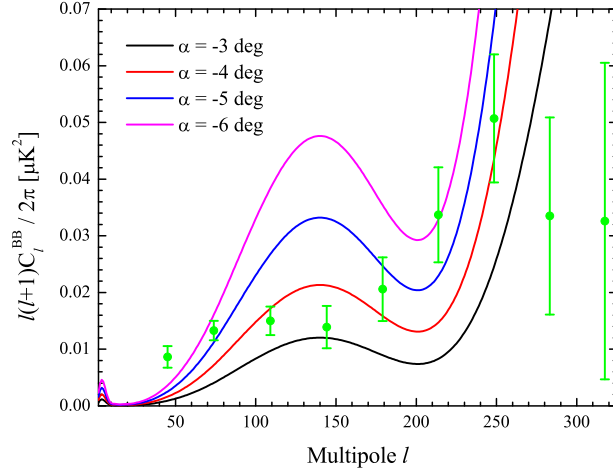


FIG. 6: Theoretical predictions of the CMB BB power spectra from the non-zero rotation angles and comparison with the BICEP2 BB data.

on  $r$  between BICEP2 and Planck, and very useful to the model building in resolving this tension.

#### Acknowledgements

We acknowledge the use of the Legacy Archive for Microwave Background Data Analysis (LAMBDA). We thank Antony Lewis, Zuhui Fan, Qing-guo Huang, Meng Su and Gongbo Zhao for helpful discussion. HL is supported in part by the National Science Foundation of China under Grant Nos. 11033005 and 11322325, by the 973 program under Grant No. 2010CB83300. J.X. is supported by the National Youth Thousand Talents Program. X.Z. is supported in part by the National Science Foundation of China under Grants Nos. 11121092, 11033005 and 11375202. This paper is supported in part by the CAS pilotB program.

- 
- [1] P. A. R. Ade *et al.* [BICEP2 Collaboration], arXiv:1403.3985 [astro-ph.CO].
  - [2] Planck Collaboration, P. A. R. Ade, *et al.*, ArXiv e-prints (2013), arXiv:1303.5076.
  - [3] A. Kehagias and A. Riotto, arXiv:1403.4811 [astro-ph.CO].
  - [4] J. Lizarraga, J. Urrestilla, D. Daverio, M. Hindmarsh, M. Kunz and A. R. Liddle, arXiv:1403.4924 [astro-ph.CO].
  - [5] R. H. Brandenberger, A. Nayeri and S. P. Patil, arXiv:1403.4927 [astro-ph.CO].
  - [6] J. -F. Zhang, Y. -H. Li and X. Zhang, arXiv:1403.7028 [astro-ph.CO].
  - [7] C. Cheng and Q. -G. Huang, arXiv:1403.5463 [astro-ph.CO].
  - [8] V. c. Miranda, W. Hu and P. Adshead, arXiv:1403.5231 [astro-ph.CO].
  - [9] M. Gerbino, A. Marchini, L. Pagano, L. Salvati, E. Di Valentino and A. Melchiorri, arXiv:1403.5732 [astro-ph.CO].
  - [10] J. Q. Xia, Y. F. Cai, H. Li, X. Zhang, arXiv:1403.7623 [astro-ph.CO].
  - [11] Y. Wang and W. Xue, arXiv:1403.5817 [astro-ph.CO].
  - [12] F. Wu, Y. Li, Y. Lu and X. Chen, arXiv:1403.6462 [astro-ph.CO].
  - [13] H. Li and J. -Q. Xia, JCAP **1211**, 039 (2012) [arXiv:1210.2037 [astro-ph.CO]].
  - [14] H. Li, J. -Q. Xia and X. Zhang, arXiv:1303.3428 [astro-ph.CO].
  - [15] J. -Q. Xia, H. Li and X. Zhang, Phys. Rev. D **88**, 063501 (2013) [arXiv:1308.0188 [astro-ph.CO]].
  - [16] A. G. Riess, *et al.*, Astrophys. J. **730**, 119 (2011).
  - [17] W. L. Freedman, *et al.*, Astrophys. J. **758**, 24 (2012).
  - [18] A. Lewis and S. Bridle, Phys. Rev. **D66**, 103511 (2002); <http://cosmologist.info/cosmomc/>.
  - [19] Planck Collaboration, P. A. R. Ade, *et al.*, ArXiv e-prints (2013), arXiv:1303.5075.
  - [20] Planck Collaboration, P. A. R. Ade, *et al.*, ArXiv e-prints (2013), arXiv:1303.5077.
  - [21] WMAP Collaboration, G. Hinshaw, *et al.*, ArXiv e-prints (2012), arXiv:1212.5226.
  - [22] P. A. R. Ade *et al.* [The POLARBEAR Collaboration], arXiv:1403.2369 [astro-ph.CO].

- [23] D. J. Eisenstein, H.-J. Seo and M. J. White, *Astrophys. J.* **664**, 660 (2007).
- [24] A. Albrecht, *et al.*, ArXiv e-prints (2006), arXiv:astro-ph/0609591.
- [25] T. Okumura, *et al.*, *Astrophys. J.* **676**, 889 (2008).
- [26] D. J. Eisenstein, *et al.*, *Astrophys. J.* **633**, 560 (2005).
- [27] F. Beutler, *et al.*, *Mon. Not. Roy. Astron. Soc.* **416**, 3017 (2011).
- [28] N. Padmanabhan, *et al.*, *Mon. Not. Roy. Astron. Soc.* **427**, 2132 (2012).
- [29] L. Anderson, *et al.*, *Mon. Not. Roy. Astron. Soc.* **428**, 1036 (2013).
- [30] N. Suzuki *et al.*, *Astrophys. J.* **746**, 85 (2012).
- [31] B. Feng, H. Li, M. Li X. Zhang, *Phys. Lett. B* 620 (2005) 27; B. Feng, M. Li, J.Q. Xia, X. Chen, X. Zhang, *Phys. Rev. Lett.* 96 (2006) 221302.
- [32] H.C. Chiang *et al.*, *Astrophys. J.* **711**, 1123 (2010).
- [33] J.Q. Xia, H. Li, X. Zhang, *Phys. Lett. B* 687 (2010) 129.
- [34] J.P. Kaufman *et al.*, [BICEP1 Collaboration], arXiv:1312.7877.
- [35] S.Y. Li *et al.*, in preparation.
- [36] M. Li and X. Zhang, *Phys. Rev. D* **78**, 103516 (2008) [arXiv:0810.0403 [astro-ph]]; V. Gluscevic, D. Hanson, M. Kamionkowski and C. M. Hirata, *Phys. Rev. D* **86**, 103529 (2012) [arXiv:1206.5546 [astro-ph.CO]].
- [37] W. Zhao, M. Li, arXiv:1403.3997.
- [38] S. Lee, G.C. Liu, K.W. Ng, arXiv:1403.5585.